Comparison of the Structural Stability of Two Homologous Toxins Isolated from the Taiwan Cobra (*Naja naja atra*) Venom[†]

T. Sivaraman, T. K. S. Kumar, K. W. Hung, and C. Yu*

Department of Chemistry, National Tsing Hua University, Hsinchu, Taiwan (R.O.C.), China

Received December 14, 1999; Revised Manuscript Received May 3, 2000

ABSTRACT: Cardiotoxin analogue III (CTX III) and cobrotoxin (CBTX) isolated from the Taiwan cobra venom (*Naja naja atra*) are structurally homologous, small molecular weight, all-β-sheet proteins, cross-linked by four disulfide bonds at identical positions. The conformational stabilities of these toxins are compared based on temperature-dependent chemical shifts and amide proton exchange kinetics using two-dimensional NMR spectroscopy. The structure of CTX III is found to be significantly more stable than that of CBTX. In both the toxins, β-strand III appears to constitute the stability core. In CTX III, the stability of the triple-stranded β-sheet domain is observed to be markedly higher than the double-stranded β-sheet segment. In contrast, in CBTX, both structural domains (double- and triple-stranded β-sheet domains) appear to contribute equally to the stability of the protein. Estimation of the free energy of exchange (ΔG_{ex}) of residues in CBTX and CTX III reveals that the enhanced stability of the structure of CTX III stems from the strong interactions among the β-strands constituting the triple-stranded β-sheet domain and also the molecular forces bridging the residues at the N- and C-terminal ends of the molecule.

Snake venoms are a mixture of many proteins, of which the cardiotoxins and neurotoxins are the most toxic (*1*−*3*). Members belonging to these two toxin groups share more than 50% homology in their amino acid sequence. Chemically, snake venom cardio- and neurotoxins are small molecular mass (∼7 kDa) proteins, cross-linked by four disulfide bonds at identical positions (*4*−*7*). Comparison of the solution structures of cardiotoxin analogue III (CTX III)[1] and cobrotoxin (CBTX, a neurotoxin) isolated from the Taiwan cobra (*Naja naja atra*) venom shows that both toxins are three-finger-shaped proteins (*8*, *9*), with three loops projecting from a globular head (Figure 1). The secondary structural elements in CBTX (*8*, *10*) and CTX III (*9*, *11*) include five β-strands arranged antiparallelly into double- and triple-stranded β-sheets (Figure 1). Interestingly, despite the high degree of similarity in their three-dimensional structures, CBTX and CTX III exhibit drastically different biological activities. CTX III displays a wide array of biological activities such as lysis of erythrocytes, contraction of cardiac muscles, selective toxicity to certain types of tumor cells, and inhibition of key enzymes such as Na^+-K^+-ATPase and protein kinase C (*2*). CBTX on the other hand, blocks nerve transmission by postsynaptically binding to the acetylcholine receptor.

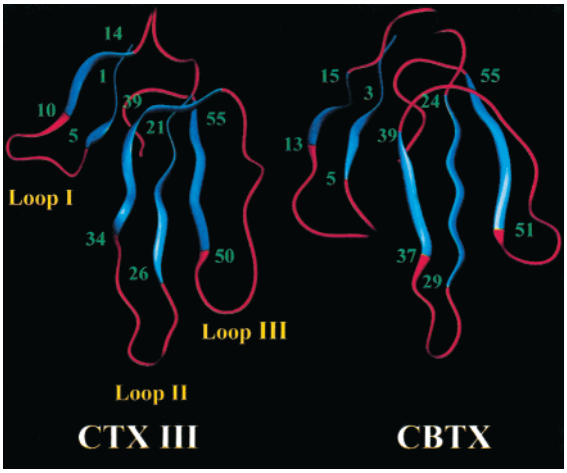

FIGURE 1: MOLSCRIPT representation of the backbone folding of CTX III and CBTX. The portions of the backbones (indicated in blue) represent the various β-strands constituting the double- and triple-stranded β-sheet domains. The numbers (indicated in green) are the amino acid residues at the extremities of the various β-strands. Appropriate orientation of the structures of CTX III and CBTX was obtained by superimposing the structures of the toxins to a minimum possible RMSD. These overlaid structures were subsequently separated on the same plane.

In the present study, we compare the structural stabilities of CBTX and CTX III using H/D exchange and temperature gradients of the amide protons using two-dimensional NMR techniques. The results obtained herein clearly demonstrate that CBTX and CTX III, despite their structural homology, differ significantly in their thermodynamic stabilities.

[†] This work was supported by research grants from the National Science Council of Taiwan and by the Dr. C. S. Tsou Memorial Medical Research Advancement Foundation.

* To whom correspondence should be addressed. E-mail: cyu@mx.nthu.edu.tw. Fax: 886-35-711082.

[1] Abbreviations: CTX III, cardiotoxin analogue III; CBTX, cobrotoxin; COSY, correlated spectroscopy; CD, circular dichroism; GdnHCl, guanidine hydrochloride; H/D exchange, hydrogen/deuterium exchange; NMR, nuclear magnetic resonance; TSP, trimethylsilylpropionate.

10.1021/bi992867j CCC: $19.00
Published on Web 07/06/2000

MATERIALS AND METHODS

CBTX and CTX III were purified from the crude Taiwan cobra venom (*Naja naja atra*) using the procedure described by Yang et al. (*12*). D_2O was purchased from Cambridge Isotope Laboratories. Ultrapure guanidine hydrochloride (GdnHCl) was purchased from Sigma Chemical Co.

Circular Dichroism. All GdnHCl and temperature-induced unfolding experiments were performed on a Jasco J720 spectropolarimeter. The unfolding of CBTX and CTX III was monitored by the ellipticity changes in the far-UV (214 nm) and near-UV (270 nm for CTX III and 285 nm for CBTX) regions. All CD measurements were carried out using 0.2 and 1 mm path length quartz cells. The GdnHCl-induced denaturation of both CTX III and CBTX (160 μM) was monitored in 0.1 M acetate buffer (prepared in D_2O and H_2O) at pH 3.4. The thermodynamic parameters of unfolding were estimated using standard methods (*13*).

NMR Spectra and Temperature Gradient Measurements. The temperature-dependent amide proton chemical shifts in CTX III and CBTX (in 10 mM acetate buffer, pH 3.4) were monitored from magnitude COSY spectra over a temperature range of 298−363 K at 5 K intervals. All NMR experiments were performed on a Bruker DMX-600 NMR spectrometer. The probe temperature was calibrated with ethylene glycol. Magnitude COSY spectra were acquired with typical data acquisition parameters of 16 transients of 1024 data points and 256 t_1 increments with water presaturation. Proton chemical shifts were referenced to an internal standard, trimethylsilylpropionate (TSP-d_4). It was ensured that the TSP-d_4 does not affect the stability of the toxins significantly. NH−C^{α}H cross-peaks in the magnitude COSY spectra of CTX III and CBTX were assigned as per the earlier assignments reported by Bhaskaran et al. (*9*) and Sivaraman et al. (*11*, for CTX III) and Yu et al. (*8*, for CBTX). Least-squares minimization of a linear equation to the chemical shift versus temperature was performed using the Kaleidagraph software (Synergy software), and the amide proton NH temperature coefficients were obtained from the gradient of the best-fit line. Temperature gradient values of various residues in CBTX and CTX III were obtained from the chemical shift changes observed in the temperature range wherein the toxin homologues do not show signs of drastic unfolding (280−323 K for CBTX and 280−343 K for CTX III). For the sake of convenience, the observed temperature gradient values are expressed on a arbitrary absolute scale. The absolute scale was obtained by neglecting the sign in the estimated temperature gradient value. The magnitude of the estimated temperature gradient values remained unaltered on the absolute scale.

Amide Proton Exchange Kinetics. H/D exchange measurements in CTX III and CBTX were monitored using the magnitude COSY spectra recorded at 25 °C (pH 3.4) using a Bruker DMX-600 NMR spectrometer. The samples for exchange kinetics of the amide protons in the proteins (CBTX and CTX III) were prepared by dissolving the lyophilized proteins in deuterated buffer at pD 3.6. The concentrations of the proteins (CBTX and CTX III) were ~2.0 mM. Cross-peak intensities were measured by volume integration. Each spectrum was referenced to nonexchangeable aromatic cross-peaks (C^{δ}H−C^{ϵ}H). Peak volumes were fit to a single-exponential function: $Y = A_o \exp^{-kt} + C$, where C is the baseline noise and takes into account the residual nondeuterated water and the threshold setting used in the intensity calculations. For some residues, the amide proton decay was fitted to the single-exponential function without inclusion of the baseline noise correction factor C (*14*). The intrinsic rate constant of exchange (k_{int}) for each amide proton was calculated using the equation for model peptides, taking into account the activation enthalpies. The protection factor (P) and the free energy of exchange (ΔG_{ex}) for the various amide protons in the protein were estimated using the method reported by Bai et al. (*15*).

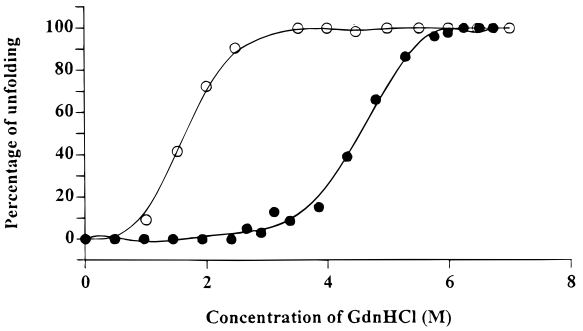

FIGURE 2: GdnHCl-induced unfolding profiles of CTX III (●) and CBTX (○). The unfolding process was monitored by the changes in the far-UV ellipticity at 214 nm. The GdnHCl denaturation experiments have been performed in 0.1 M acetate buffer, pH 3.4. The "*m*" values (which is a measure of the cooperativity of the unfolding process) for the GdnHCl-induced unfolding process of CTX III and CBTX are estimated to be 0.88 and 1.37 kcal·mol^{-1}·M^{-1}, respectively. In both toxins, the free energies of unfolding in D_2O and H_2O are similar.

RESULTS AND DISCUSSION

Equilibrium Unfolding. The GdnHCl-induced unfolding of CTX III and CBTX monitored by changes in the 214 nm ellipticity (signifying the secondary structure perturbations) is depicted in Figure 2. The GdnHCl-induced unfolding of both toxins is reversible. CTX III and CBTX cooperatively and completely unfold with a C_m of 4.7 and 1.67 M, respectively. The free energies of unfolding of CBTX and CTX III in the absence of the denaturant (ΔG_u) are estimated to be 2.27 and 4.16 kcal/mol, respectively.

The thermal unfolding of CTX III and CBTX monitored by far-UV circular dichroism (214 nm) shows that both CBTX and CTX III unfold reversibly with a T_m of 333 and 343 K, respectively. Thus, the results of the equilibrium unfolding experiments clearly suggest that the structure of CTX III is thermodynamically more stable than that of CBTX.

Temperature Gradient Measurements. Temperature gradient measurements are useful to probe solvent accessibilities of residues and also to monitor the conformational changes accompanying a temperature-induced unfolding process (*16*−*18*). In principle, amide protons show marked changes in their chemical shift values with temperature. Amide protons which are not hydrogen bonded and exposed to the solvent show larger changes in the chemical shift values than those which are involved in hydrogen bonding in the protein molecule. In general, the magnitude of the temperature gradient estimate is inversely related to the relative stability of the residue in a protein. The temperature gradients of

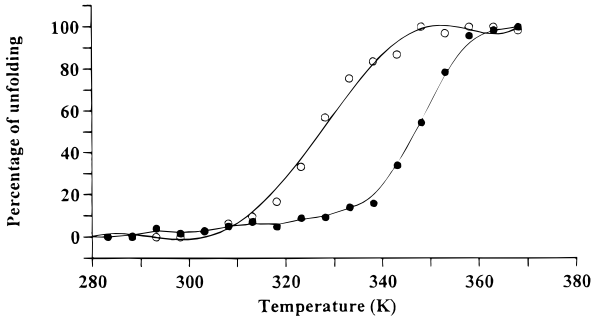

FIGURE 3: Thermal unfolding profiles of CTX III (●) and CBTX (○). The unfolding of the toxin homologues was monitored by the ellipticity changes at 214 nm. The T_m values of CBTX and CTX III were estimated to be 330 and 343 K, respectively.

amide protons serve as indicators for hydrogen bonding, and, in general, values higher than 4.5 ppb/K are indicative of the involvement of the amide proton(s) in intramolecular hydrogen bonding (*16*). To understand the molecular basis underlying the vast difference(s) in the conformational stabilities of CBTX and CTX III, in the present study, we compare the temperature gradients of the amide protons of various residues in these two structurally homologous toxins.

Spectral assignments of the NH−C$^{\alpha}$H cross-peaks in these structurally homologous toxins (CBTX and CTX III) are available from our earlier studies (*9*−*11*). Magnitude COSY spectra of both toxins are well dispersed (Supporting Information Figures S1 and S2), and we could unambiguously monitor the temperature-dependent chemical shifts of 41 and 38 amide protons of CTX III and CBTX, respectively. Thermal unfolding of both the toxins was found to be reversible even at the high concentrations used (2.0 mM) in the magnitude COSY experiments (Supporting Information Figures S1 and S2). Most of the amide protons in CTX III in the structured region(s) exhibit temperature gradient values (<4.5 ppb/K) lower than those in the unstructured portion(s) of the toxin molecule (Figure 4). The average temperature gradients of residues comprising the double- and triple-stranded β-sheet domains are estimated to be 4.13 and 3.51 ppb/K, respectively. Among the three β-strands (β-strands III, IV, and V) constituting the triple-stranded β-sheet domain, β-strand III exhibits the least average temperature gradient value of 2.68 ppb/K. In fact, all the residues (Cys21−Met26) comprising β-strand III exhibit temperature gradient values lower than 3.5 ppb/K (Figure 4). Comparison of the temperature gradient data of the β-strands in CTX III indicates that β-strand III constitutes the most stable core of the toxin molecule. Some of the residues belonging to the structured regions of the molecule show higher temperature (>4.5 ppb/K) gradient values. For example, Tyr11 and Thr13, which are located in β-strand II, show abnormally high temperature gradient values (>6.0 ppb/K). The double-stranded β-sheet in CTX III exhibits a small twist in the backbone-spanning residues located in β-strand II (*9*, *11*), leading to increased solvent exposure of the amide protons of Tyr11 and Thr13. This results in the weakening of the interstrand hydrogen bonding with the partnering carbonyl groups in β-strand I. Similarly, Arg36 and Cys38, located in β-strand IV, show abnormally high temperature gradient values (>4.5 ppb/K). The occurrence of two proline residues at positions 30 and 33 in CTX III prevents the amide protons of Arg36 and Cys38 from fostering hydrogen bonds with

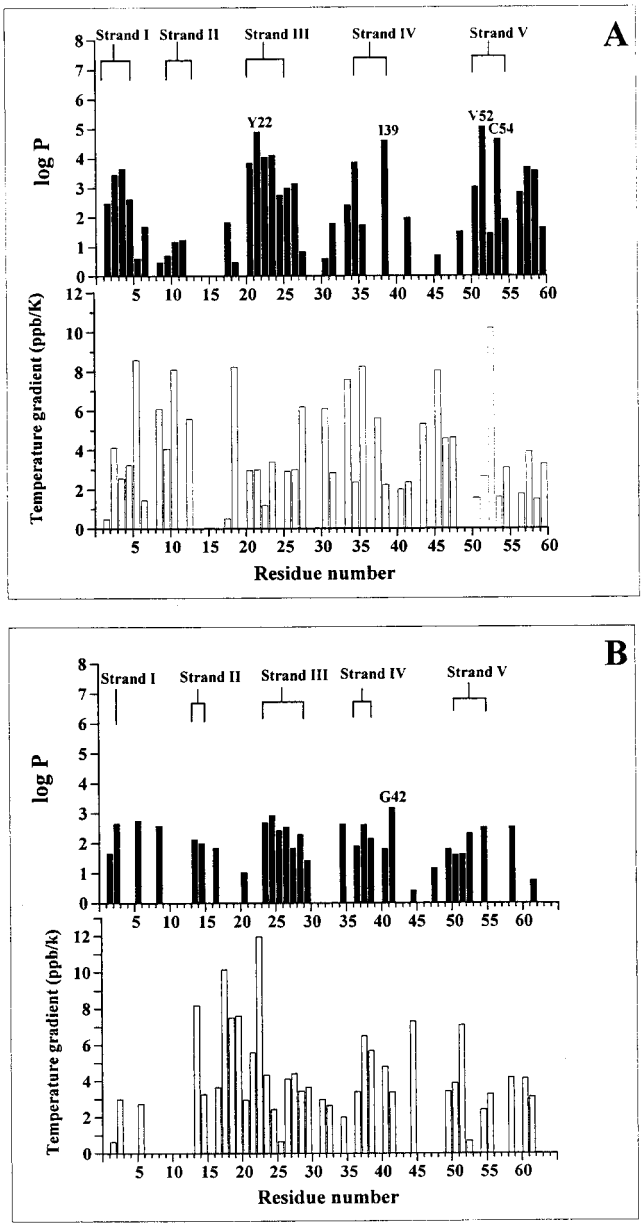

FIGURE 4: Comparison of the protection factors (black bars) and the amide proton temperature gradients (white bars) of various residues in (A) CTX III and (B) CBTX. It could be deduced that amide protons of Tyr22, Cys23, Met24, Ile39, Val52, and Cys54 show extraordinarily high protection factors in CTX III. With the exception of Gly42 (P = 1500), none of the residues in CBTX exhibit protection factor values greater than 1000.

the carbonyl groups of residues located in the double-stranded domain. Most of the non-hydrogen-bonded residues in the CTX III molecule exhibit temperature gradient values higher than 4.5 ppb/K (Figure 4), the most notable exception being Lys18, which displays an exceptionally low temperature gradient value of 0.50 ppb/K (Figure 4). Lys18 is located in the head region of the CTX III molecule, which is excessively cross-linked by disulfide bonds. The high degree of cross-linking probably renders residues located in the head portion rigid, and consequently the molecular environment around the amide proton of Lys18 undergoes limited change with the increase in temperature. However, in the absence of strong experimental evidence, our explanation on the observed anomalous temperature gradient value of the amide proton of Lys18 remains a conjecture.

It is interesting to note that the residues spanning the C-terminal segment (Asp57−Asn60) in CTX III show temperature gradient values lower than 4.0 ppb/K. The C-terminal segment in CTX III is cross-linked by a disulfide bond between Cys54 and Cys59. In addition, two hydrogen bonds between the NH- groups of Cys59 and Arg58 and the carbonyl groups of Lys2 and Asn4, respectively, tether the N- and C-terminal ends of the CTX III molecule. In addition, the side chain amide group of Asn60 is also known to have long-range interactions with the backbone carbonyl groups of Cys21 and Tyr22. The presence of a disulfide bond (between Cys54 and Cys59) and a strong network of backbone interactions between the N- and C-terminal ends appears to contribute significantly to the structural stability of the CTX III molecule.

There appears to be little or no difference in the average temperature gradient values of the double (4.37 ppb/K) and triple (4.38 ppb/K) stranded β-sheet domains in CBTX III. This is in marked contrast to CTX III, wherein the triple-stranded domain shows a lower average temperature gradient value (3.5 ppb/K) than the double-stranded β-sheet (4.13 ppb/K) segment. Among the three β-strands (β-strands III, IV, and V) constituting the triple-stranded β-sheet domain in CBTX, β-strand III shows the least average temperature gradient value (3.24 ppb/K). Interestingly, the average temperature gradient values of all the β-strands in CBTX are relatively higher than those of the corresponding β-strands in CTX III, implying that the secondary structure of CBTX is less stable than that of CTX III. The average temperature gradient value of the C-terminal segment in CBTX, spanning residues Thr56−Asn62, is marginally lower than that in CTX III (4.0 ppb/K). Similar to CTX III, the C-terminal segment in CBTX is stabilized through a disulfide bond between Cys56 and Cys60, and the N- and C-terminal ends of the toxin molecule are bridged by a weak hydrogen bond between Glu2NH and Arg59CO. The marginally higher average temperature gradient value of the C-terminal segment in CBTX (as compared to in CTX III) could be due to a lesser number of structural interactions linking the N- and the C-termini of the toxin molecule.

Interestingly, the residues present at the tip of loop II (residues 30−35) in CBTX unexpectedly show a low average temperature gradient value of 2.83 ppb/K. None of the amide protons of the residues at the tip of loop II are involved in hydrogen bonding. This aspect is corroborated by the low protection factors of the residues located in this segment. The theoretical basis for the temperature-dependent chemical shifts is not yet completely understood, and important deviations are known to arise from local electric fields (like ring current effects of spatially close aromatic side chains or local fields from charged neighbors) or due to the presence of proline residues in the protein segment of interest (*19*−*22*). Interestingly, the amino acid stretch between residues 30 and 35 is rich in charged and aromatic residues. In fact, except for Gly34, all the remaining residues in this stretch are either aromatic or charged. The solution structure of CBTX shows that residues 30−35 are encircled by positively charged residues and the aromatic rings contributed by Trp29 and Tyr25. These structural features could be cumulatively or individually responsible for the anomalous temperature gradient values of the non-hydrogen-bonded residues located at the tip of loop II in CBTX.

Amide−Proton Exchange Kinetics. Hydrogen/deuterium (H/D) exchange studies provide useful information on the relative solvent accessibility of various amide protons (*23*). These differences in the exchange rates of amide protons are a direct measure of the local rigidity or flexibility in the protein molecule, and hence H/D exchange studies provide a detailed, residue level information on the structural stability of protein(s).

The amide proton exchange kinetics of 40 residues in CTX III were monitored. The majority of the residues not involved in secondary structure formation in CTX III show weak protection ($P < 100$) against exchange. Interestingly, the C-terminal segment (residues 57−59) shows relatively high ($P > 500$) protection. The average protection factor of the residues in the triple-stranded β-sheet domain ($P \sim 22\,000$) is far greater than that of the double-stranded β-sheet segment ($P \sim 1000$). It appears that the stability of CTX III is largely due to the triple-stranded β-sheet domain. Several residues in the triple-stranded β-sheet domain, such as Tyr22, Lys23, Met24, Ile39, Val52, and Cys54, show extraordinarily high protection ($P > 10\,000$) against H/D exchange (Figure 4). β-Strand III, comprising Tyr22, Lys23, and Met24, is encircled by a hydrophobic cluster comprised of Leu6, Val17, Phe25, Val32, and Val34 (*9*, *11*). This nonpolar core appears to effectively insulate the amide protons of Tyr22, Lys23, and Met24 from solvent (D_2O) exchange. Similarly, the relatively high protection of Tyr22 ($P > 80\,000$) could be attributed to the masking of its amide proton by the nonpolar side chains of Ile39 and Val41. Ile39 and Cys54 are the other two residues that show strong protection ($P > 40\,000$), and are located in close proximity to the head region (which is cross-linked by four disulfide bonds) of the CTX III molecule. In addition, these two residues are involved in hydrogen bonding with the carbonyl groups of Leu20 and Cys21. These structural features possibly account for the high protection of Ile39 and Cys54 (Figure 4).

The amide proton of Val52 shows the strongest protection ($P > 117\,000$) against H/D exchange. Critical analysis of the solution structure of CTX III shows that (1) the amide proton of Val52 is hydrogen bonded to the carbonyl group of Met 24, (2) the amide proton of Val52 is sandwiched between the phenolic groups of Tyr22 and Tyr51 (as exemplified by the strong ring current effects experienced on the methyl protons of Val52), and (3) the disulfide bonds between Cys42 and Cys53 and between Cys54 and Cys59 tightly pack β-strand V, comprising Val52. These structural features almost impregnate the amide proton of Val52 and could be collectively responsible for its slow exchange with the solvent (D_2O).

In contrast to CTX III, we could monitor the exchange kinetics of only 29 of the 58 total amide protons in CBTX. With the exception of Gly42 ($P = 1500$), the protection factors of the remaining amide protons in CBTX are less than 1000 (Figure 4). The high protection factor value of Gly42 could be attributed to the presence of a type II β-turn between Gly42NH and the carbonyl group of Val46. Among the five β-strands, β-strand III shows the highest average protection factor value of 373, indicating that this β-strand is the most stable core in the structure of CBTX. However, the average protection factor of β-strand III in CBTX is lower than that observed in CTX III. In addition, the average protection factor of residues in the C-terminal segment of

Table 1: Average Free Energy (kcal/mol) of Exchange of Amide Protons in Various Portions of the Structures of CBTX and CTX III

proteins/structural context	structured region	unstructured region	double strand		triple strand			
			strand I	strand II	strand III	strand IV	strand V	C-terminal
CTX III	4.17	2.27	4.16	1.39	5.15	4.64	4.40	4.00
			(2.97)[a]			(4.17)		
CBTX	3.10	2.52	3.28	2.93	3.35	3.04	2.76	2.26
			(3.09)			(3.10)		

[a] The numbers in parentheses represent the average free energy values of the double- and triple-stranded β-sheet domains.

CBTX is significantly lower than that of the corresponding region in CTX III. As mentioned earlier, the presence of a lesser number of structural contacts between the N- and C-terminal ends of the CBTX molecule probably accounts for the lower average stability of the C-terminal segment in CBTX.

Comparison of the Structural Stabilities of CBTX and CTX III. Recently, the conformational stabilities of various proteins calculated from H/D exchange rate constants have been shown to be in excellent agreement with those determined by traditional optical spectroscopic methods (*25*−*27*). In this context, the H/D exchange studies permit us to estimate the free energy of exchange of individual amide protons in the toxin homologues, and such information is useful to understand the molecular basis for the enhanced structural stability of CTX III as compared to CBTX.

Both toxins contain five β-strands which are arranged into antiparallel double- and triple-stranded β-sheet domains. In this context, it would be interesting to compare the stabilities of the individual secondary structural elements in CTX III and CBTX, in terms of the free energy of exchange (ΔG_{ex}). The order of stability of the various β-strands in CTX III is β-strand III (5.15 kcal/mol), β-strand IV (4.64 kcal/mol), β-strand V (4.40 kcal/mol), β-strand I (4.16 kcal/mol), and β-strand II (1.39 kcal/mol, Table 1). It appears that β-strand III constitutes the most stable core of the protein (CTX III). In CBTX, the stability of the various β-strands is in the order: β-strand III (3.35 kcal/mol), β-strand I (3.25 kcal/mol), β-strand IV (3.04 kcal/mol) β-strand II (2.93 kcal/mol), and β-strand V (2.76 kcal/mol). With the exception of β-strand II, the stabilities of all other β-strands in CTX III are significantly higher than their counterparts in CBTX, and this feature probably accounts (to a large extent) for the greater conformational stability of CTX III as compared to CBTX. Interestingly, there are notable difference(s) in the contribution of the double- and triple-stranded β-sheet domains (toward the global stability) in CTX III and CBTX. In CTX III, the average free energy of exchange of residues located in the triple-stranded β-sheet domain (4.17 kcal·mol^{-1}) far exceeds that of the double-stranded (2.97 kcal·mol^{-1}) domain. In contrast, in CBTX, both the double-stranded (ΔG_{ex} = 3.09 kcal·mol^{-1}) and triple-stranded β-sheet domains (3.10 kcal·mol^{-1}) appear to contribute equally to the overall stability of the toxin (Table 1).

The solution structures of CTX III and CBTX exhibit significant differences in the organization of the C-terminal segment. The ΔG_{ex} values of the residues in the C-terminal segment in CTX III and CBTX are 4.00 and 2.26 kcal/mol, respectively (Table 1). The free energy estimations clearly suggest that the differences in the structural interactions among the residues at the N- and C-termini in CBTX and CTX III also contribute significantly to the overall thermodynamic stabilities of the toxin homologues.

The results of the present study clearly demonstrate that CTX III and CBTX, despite being structurally very similar, differ significantly in their thermodynamic stabilities. Cloning of these two structurally homologous proteins is underway to validate some of the findings reported in this study (*28*).

SUPPORTING INFORMATION AVAILABLE

Two-dimensional magnitude COSY spectra of CTX III at various temperatures (Figure S1) and two-dimensional magnitude COSY spectra of CBTX at various temperatures (Figure S2) (2 pages). This material is available free of charge via the Internet at http://pubs.acs.org.

REFERENCES

1. Kumar, T. K. S., Pandian, S. K., Sailam, S., and Yu, C. (1998) *J. Toxicol. Toxin Res. 17*, 183−212.
2. Kumar, T. K. S., Jayaraman, G., Lee, C. S., Arunkumar, A. I., Sivaraman, T., Samuel, D., and Yu, C. (1997) *J. Biomol. Struct. Dyn. 15*, 430−463.
3. Kumar, T. K. S., Lee, C. S., and Yu, C. (1996) in *Natural Toxins* (Singh, B. R., and Tu, A. T., Eds.) pp 114−129, Plenum Press, New York.
4. Jang, J. Y., Kumar, T. K. S., Jayaraman, G., Yang, P. W., and Yu, C. (1997) *Biochemistry 36*, 14635−14641.
5. Sivaraman, T., Kumar, T. K. S., Chang, D. K., Lin, W. Y., and Yu, C. (1998) *J. Biol. Chem. 273*, 10181−10189.
6. Jayaraman, G., Kumar, T. K. S., and Yu, C. (1999) *J. Biol. Chem. 274*, 17869−17875.
7. Sivaraman, T., Kumar, T. K. S., Tu, Y. T., Peng, H. J., and Yu. C. (1999) *Arch. Biochem. Biophys. 363*, 107−115.
8. Yu, C., Bhaskaran, R., Chaung, L. C., and Yang, C. C. (1993) *Biochemistry 32*, 2131−2136.
9. Bhaskaran, R., Huang, C. C., Chang, D. K., and Yu, C. (1994) *J. Mol. Biol. 235*, 291−301.
10. Yu, C., Lee, C. S., Wang, C. Y., and Shei, Y. R. (1990) *Eur. J. Biochem. 193*, 789−799.
11. Sivaraman, T., Kumar, T. K. S., Huang, C. C., and Yu, C. (1998) *Biochem. Mol. Biol. Int. 44*, 29−39.
12. Yang, C. C., King, R., and Sun, T. P. (1981) *Toxicon 19*, 645−659.
13. Tanford, C. (1968) *Adv. Protein Chem. 23*, 121−282.
14. Sivaraman, T., Kumar, T. K. S., and Yu, C. (1999) *Biochemistry 38*, 9899−9905.
15. Bai, Y., Millne, J. S., Mayne, L., and Englander, S. W. (1995) *Proteins: Struct., Funct., Genet. 17*, 75−86.
16. Baxter, N. J., and Williamson, M. P. (1997) *J. Biomol. NMR 9*, 359−369.
17. Dyson, H. J., Rance, M., Houghten, R. A., Lerner, R. A., and Wright, P. E. (1988) *J. Mol. Biol. 201*, 161−200.
18. Baxter, N. J., Hosszu, L. P., Waltho, J. P., and Williamson, M. P. (1998) *J. Mol. Biol. 284*, 1625−1639.
19. deDios, A. C., Pearson, J. G., and Oldfield, E. (1993) *Science 260*, 1491−1496.
20. deDios, A. C., Pearson, J. G., and Oldfield, E. (1993) *J. Am. Chem. Soc. 115*, 9768−9773.
21. Laws, D. D., de Dios, A. C., and Old field, E. (1995) *J. Biomol. NMR 3*, 607−612.

22. Howarth, O. W., and Lilley, D. M. J. (1978) *Prog. NMR Spectrosc. 12*, 1−40.
23. Li, R., and Woodward, C. (1999) *Protein Sci. 8*, 1571−1591.
24. Perret, S., Clarke, J., Hounston, A. M., and Fersht, A. R. (1995) *Biochemistry 34*, 9288−9299.
25. Beatrice, M. P., Despointes, H., Scholtz, J. M., and Pace, C. N. (1999) *Nat. Struct. Biol. 6*, 910−912.
26. Bai, Y. (1999) *J. Biomol. NMR 15*, 65−70.
27. Bai, Y. (1999) *Proc. Natl. Acad. Sci. U.S.A. 96*, 477−480.
28. Kumar, T. K. S., Yang, P. W., Lin, S. H., Wu, C. Y., Lei, B., Lo, S. J., Tu, S. C., and Yu, C. (1996) *Biochem. Biophys. Res. Commun. 219*, 450−456.

BI992867J